慶應義塾大学学術情報リポジトリ
Keio Associated Repository of Academic resouces

Title	Large dddy simulation for the dynamic Clark model with an anisotropic filter
Sub Title	
Author	小林, 宏充(Hiromichi, Kobayashi)
Publisher	慶應義塾大学日吉紀要刊行委員会
Publication year	2004
Jtitle	慶應義塾大学日吉紀要. 自然科学 No.36 (2004. 9) ,p.15- 26
JaLC DOI	
Abstract	The asymptotic behavior and the performance of the dynamic Clark model with an anisotropic filter are analytically and numerically revealed in comparison with the dynamic Smagorinsky model and the dynamic mixed model. In the dynamic Clark model, the change of the isotropic filter-width for the Clark term to the anisotropic one makes it possible to apply to turbulent channel flows. Then, the near-wall scaling of the model coefficient for the dynamic Clark model is also corrected as y3. The performance of the dynamic Clark model is the almost same as that of the dynamic mixed model, which is better than the dynamic Smagorinsky model.
Notes	
Genre	Departmental Bulletin Paper
URL	https://koara.lib.keio.ac.jp/xoonips/modules/xoonips/detail.php?koara_id=AN10079809-20040930-0015

慶應義塾大学学術情報リポジトリ(KOARA)に掲載されているコンテンツの著作権は、それぞれの著作者、学会または出版社/発行者に帰属し、その権利は著作権法によって保護されています。引用にあたっては、著作権法を遵守してご利用ください。

The copyrights of content available on the KeiO Associated Repository of Academic resources (KOARA) belong to the respective authors, academic societies, or publishers/issuers, and these rights are protected by the Japanese Copyright Act. When quoting the content, please follow the Japanese copyright act.

Hiyoshi Review of Natural Science
Keio University No. 36, 15–25 (2004)

Large Eddy Simulation for the dynamic Clark model with an anisotropic filter

Hiromichi KOBAYASHI

Summary——The asymptotic behavior and the performance of the dynamic Clark model with an anisotropic filter are analytically and numerically revealed in comparison with the dynamic Smagorinsky model and the dynamic mixed model. In the dynamic Clark model, the change of the isotropic filter-width for the Clark term to the anisotropic one makes it possible to apply to turbulent channel flows. Then, the near-wall scaling of the model coefficient for the dynamic Clark model is also corrected as y^3. The performance of the dynamic Clark model is the almost same as that of the dynamic mixed model, which is better than the dynamic Smagorinsky model.
Key words : large eddy simulation, turbulence, numerical simulation

1. Introduction

Large eddy simulation (LES) is one of turbulent models.[1, 2] In LES larger properties than a grid-scale (GS) are directly calculated, whereas smaller properties than the GS, that is, properties of a subgrid-scale (SGS) are modeled. The velocity and the pressure fields (f) are decomposed into the GS and the SGS components using a filtering procedure:

$$\overline{f}(\boldsymbol{x}) = \int_{\infty}^{\infty} f(\boldsymbol{x}')\overline{G}(\boldsymbol{x}, \boldsymbol{x}')\, d\boldsymbol{x}', \tag{1}$$

where $\overline{G}(\boldsymbol{x})$ denotes the filter function, and $\overline{f}$ is the filtered or the GS component. In the filtered Navier-Stokes equation for the GS flow field, there appears the SGS stress tensor τ_{ij}, which is defined by

$$\tau_{ij} \equiv (\overline{u_i u_j} - \overline{u}_i \overline{u}_j)_{\Sigma}, \tag{2}$$

where u_i is the i-th component of velocity vector, the overbar $\overline{u}$ denotes the GS component of u, hereafter $(A_{ij})_{\Sigma}$ means the traceless matrix $A_{ij} - \delta_{ij} A_{aa}/3$, and the summation convention is used for repeated

小林宏充, 慶應義塾大学日吉物理教室（〒223-8521 横浜市港北区日吉４－１－１）: Dept. of Phys., Keio Univ., 4-1-1, Hiyoshi, Kohoku-ku, Yokohama, 223-8521, Japan. [Received]

subscripts. The SGS stress tensor τ_{ij} can be decomposed into the Leonard term L_{ij}, the cross term C_{ij} and the SGS Reynolds stress R_{ij} as follows:

$$\tau_{ij} = (L_{ij} + C_{ij} + R_{ij})_{\Sigma}, \tag{3}$$

$$L_{ij} \equiv \overline{\overline{u}_i \overline{u}_j} - \overline{u}_i \overline{u}_j, \tag{4}$$

$$C_{ij} \equiv \overline{\overline{u}_i u'_j + u'_i \overline{u}_j}, \tag{5}$$

$$R_{ij} \equiv \overline{u'_i u'_j}, \tag{6}$$

where u'_i denotes the SGS part of u_i, defined by

$$u'_i \equiv u_i - \overline{u}_i. \tag{7}$$

The most famous and useful model is the Smagorinsky model[3]. However, some modified models to obtain higher performance and accuracy are proposed. Clark, Ferziger, and Reynolds[4] proposed a SGS model in LES, which is composed of two parts: one is the eddy-viscosity representation for the SGS Reynolds stress, and the other is the Clark term $L_{ij} + C_{ij}$ for the sum of the Leonard and the cross terms, which is obtained by a Taylor expansion of the velocity fields. This model is called the Clark model, the gradient model, or the tensor diffusivity model. Bardina, Ferziger, and Reynolds[5] proposed a SGS model which is composed of also two parts: one is the eddy-viscosity representation, and the other is the similarity term $\overline{\overline{u}_i \overline{u}_j} - \overline{\overline{u}}_i \overline{\overline{u}}_j$, which is based on a scale similarity of the velocity fields $u_i \approx \overline{u}_i$. This model is called the mixed model or the similarity model. The SGS eddy viscosities in the Clark model and the mixed model are modeled by the same expression as the Smagorinsky model[3], so that each model "constant" (the Smagorinsky constant) needs to be tuned depending upon the turbulent flow to be simulated. Vreman, Geurts, and Kuerten[6,7] proposed the dynamic Clark model (DCM) based on the dynamic procedure,[8] and found its better performance for the turbulent mixing layer. Shimomura[10] pointed out from a mathematical view point that the (dynamic) Clark model is consistent with the constraint of asymptotic material frame indifference (AMFI), while most of the existing models including the dynamic Smagorinsky model (DSM)[8] and the dynamic mixed model (DMM)[9] are not. In fact, Kobayashi and Shimomura[11] have recently demonstrated a good performance of the DCM and an unphysical behavior of the DSM in LES of rotating homogeneous turbulence.

Until recently, the DCM has not been applied to LES of incompressible turbulent channel flows. For the DCM with an isotropic filter it has been revealed that the reason is neither a negative SGS eddy viscosity nor an incorrect near-wall scaling, but a negative effective viscosity in the viscous sublayer for the Clark term.[12] Vreman commented that although above discussion is true for the DCM with isotropic filters, for the DCM with anisotropic filters such as channel flows the expression of the Clark term should be changed to the anisotropic version as follows:[13]

The isotropic Clark term:

$$\frac{\overline{\Delta}^2}{12}\left(\frac{\partial \overline{u}_i}{\partial x_1}\frac{\partial \overline{u}_j}{\partial x_1}+\frac{\partial \overline{u}_i}{\partial x_2}\frac{\partial \overline{u}_j}{\partial x_2}+\frac{\partial \overline{u}_i}{\partial x_3}\frac{\partial \overline{u}_j}{\partial x_3}\right), \tag{8}$$

The anisotropic Clark term:

$$\frac{1}{12}\left(\overline{\Delta}_1^2\frac{\partial \overline{u}_i}{\partial x_1}\frac{\partial \overline{u}_j}{\partial x_1}+\overline{\Delta}_2^2\frac{\partial \overline{u}_i}{\partial x_2}\frac{\partial \overline{u}_j}{\partial x_2}+\overline{\Delta}_3^2\frac{\partial \overline{u}_i}{\partial x_3}\frac{\partial \overline{u}_j}{\partial x_3}\right), \tag{9}$$

where $\overline{\Delta}$ the isotropic filter width, $(x_1, x_2, x_3) = (x, y, z)$, $(\overline{\Delta}_1, \overline{\Delta}_2, \overline{\Delta}_3) = (\overline{\Delta}_x, \overline{\Delta}_y, \overline{\Delta}_z)$, the GS velocities $(\overline{u}_1, \overline{u}_2, \overline{u}_3) = (\overline{u}, \overline{v}, \overline{w})$, and x, y and z denote the streamwise, the normal and the spanwise directions of the channel flow, respectively. The relations between the isotropic and the anisotropic filter width are as follows:

The isotropic filter width:

$$\overline{\Delta} = \overline{\Delta}_1 = \overline{\Delta}_2 = \overline{\Delta}_3 . \tag{10}$$

The anisotropic filter width:

$$\overline{\Delta} \neq \overline{\Delta}_1 \neq \overline{\Delta}_2 \neq \overline{\Delta}_3 , \qquad \overline{\Delta} = (\overline{\Delta}_1\overline{\Delta}_2\overline{\Delta}_3)^{1/3} , \tag{11}$$

where the last relation is usually adopted for the Gaussian or the top hat filter.[8] His comment is completely correct, then in its response it has been mentioned that the Clark term for the DCM with anisotropic filters and the similarity term for the DMM have the same leading term up to the accuracy of $O(\overline{\Delta}_m^2)$, where $\overline{\Delta}_m$ is the maximum filter width.[14]

In the present paper, the near-wall scaling of the model coefficient for the DCM with an anisotropic filter is revealed. Furthermore, the performance of the DCM with an anisotropic filter, the DMM, and the DSM is compared in actual LES.

In Sec. 2., the model expressions of the DSM, the DCM, and the DMM for the SGS stress tensor are described. Moreover, the asymptotic behaviors of the DSM, the DCM, and the DMM in the viscous sublayer of turbulent channel flows are given in Sec. 3.. In Sec. 4., the analytical results are numerically checked for a turbulent channel flow with LES at $Re_\tau = 590$. Section 5. presents the conclusions that can be drawn fromthe present work.

2. Expressions of Dynamic Models

First, let us remember the model expressions of the DSM, the DCM, and the DMM for the SGS stress tensor. The derivation is referred to, for example, Kobayashi and Shimomura.[11] In the following, C_D is the model parameter, and is denoted for each model as C_{DSM}, C_{DCM}, and C_{DMM} for the DSM, the DCM,

and the DMM, respectively. They are dynamically evaluated by using the least squared method.[15] The GS rate of strain tensor $\overline{S}_{ij}$ and its magnitude $|\overline{S}|$ are defined by

$$\overline{S}_{ij} = \frac{1}{2}\left(\frac{\partial \overline{u}_i}{\partial x_j} + \frac{\partial \overline{u}_j}{\partial x_i}\right), \tag{12}$$

$$|\overline{S}| = \sqrt{2\overline{S}_{ij}\,\overline{S}_{ij}}. \tag{13}$$

$\widehat{f}$ is the test-filtered field of f, and $\widehat{\Delta}$ is the test-filter width. The filter width and the test-filter width are related to the double-filter width $\widehat{\overline{\Delta}}$ by

$$\widehat{\overline{\Delta}}^{\,2} = \overline{\Delta}^{\,2} + \widehat{\Delta}^{\,2}, \qquad \widehat{\Delta} = (\widehat{\Delta}_1\widehat{\Delta}_2\widehat{\Delta}_3)^{1/3}, \qquad \widehat{\overline{\Delta}} = (\widehat{\overline{\Delta}}_1\widehat{\overline{\Delta}}_2\widehat{\overline{\Delta}}_3)^{1/3}, \tag{14}$$

In the following, the repeated subscript (a) means the special summation convention:

$$\frac{1}{12}\left(\overline{\Delta}_{(a)}^{\,2}\frac{\partial \overline{u}_i}{\partial x_{(a)}}\frac{\partial \overline{u}_j}{\partial x_{(a)}}\right) = \frac{1}{12}\left(\overline{\Delta}_1^{\,2}\frac{\partial \overline{u}_i}{\partial x_1}\frac{\partial \overline{u}_j}{\partial x_1} + \overline{\Delta}_2^{\,2}\frac{\partial \overline{u}_i}{\partial x_2}\frac{\partial \overline{u}_j}{\partial x_2} + \overline{\Delta}_3^{\,2}\frac{\partial \overline{u}_i}{\partial x_3}\frac{\partial \overline{u}_j}{\partial x_3}\right). \tag{15}$$

The DSM:

$$\tau_{ij} = -2C_{DSM}\overline{\Delta}^{\,2}|\overline{S}|\,\overline{S}_{ij}, \tag{16}$$

$$C_{DSM} = \frac{\langle \mathcal{L}_{ij}\, M_{ij}\rangle}{\langle M_{ij}\, M_{ij}\rangle}. \tag{17}$$

The DCM:

$$\tau_{ij} = \left(\frac{\overline{\Delta}_{(a)}^{\,2}}{12}\frac{\partial \overline{u}_i}{\partial x_{(a)}}\frac{\partial \overline{u}_j}{\partial x_{(a)}}\right)_{\Sigma} - 2C_{DCM}\overline{\Delta}^{\,2}|\overline{S}|\,\overline{S}_{ij}, \tag{18}$$

$$C_{DCM} = \frac{\langle (\mathcal{L}_{ij} + \mathcal{G}_{ij})\, M_{ij}\rangle}{\langle M_{ij}\, M_{ij}\rangle}. \tag{19}$$

The DMM:

$$\tau_{ij} = (\overline{\overline{u}_i\,\overline{u}_j} - \overline{\overline{u}}_i\,\overline{\overline{u}}_j)_{\Sigma} - 2C_{DMM}\overline{\Delta}^{\,2}|\overline{S}|\,\overline{S}_{ij}, \tag{20}$$

$$C_{DMM} = \frac{\langle (\mathcal{L}_{ij} + \mathcal{H}_{ij})\, M_{ij}\rangle}{\langle M_{ij}\, M_{ij}\rangle}. \tag{21}$$

In the above expressions,

$$\mathcal{L}_{ij} = \left(\widehat{\overline{u}_i \overline{u}_j} - \widehat{\overline{u}}_i \widehat{\overline{u}}_j\right)_{\Sigma}, \tag{22}$$

$$M_{ij} = 2\overline{\Delta}^2 |\widehat{\overline{S}}| \widehat{\overline{S}}_{ij} - 2\widehat{\overline{\Delta}}^2 |\widehat{\overline{S}}| \widehat{\overline{S}}_{ij}, \tag{23}$$

$$\mathcal{G}_{ij} = \left(\frac{\overline{\Delta}^2_{(a)}}{12} \widehat{\frac{\partial \overline{u}_i}{\partial x_{(a)}}} \widehat{\frac{\partial \overline{u}_j}{\partial x_{(a)}}} - \frac{\widehat{\overline{\Delta}}^2_{(a)}}{12} \frac{\partial \widehat{\overline{u}}_i}{\partial x_{(a)}} \frac{\partial \widehat{\overline{u}}_j}{\partial x_{(a)}} \right)_{\Sigma}, \tag{24}$$

$$\mathcal{H}_{ij} = \left(\widehat{\widehat{\overline{u}_i \overline{u}_j}} - \widehat{\overline{\overline{u}}_i \overline{\overline{u}}_j}\right)_{\Sigma} - \left(\widehat{\widehat{\overline{u}_i \overline{u}_j}} - \widehat{\overline{\overline{u}}}_i \widehat{\overline{\overline{u}}}_j\right)_{\Sigma}. \tag{25}$$

3. Asymptotic Behaviors

Next, the asymptotic behaviors of the DSM, the DCM, and the DMM in the viscous sublayer of turbulent channel flows are studied. The coordinate $(x_1, x_2, x_3) = (x, y, z)$ and the GS velocities $(\overline{u}_1, \overline{u}_2, \overline{u}_3) = (\overline{u}, \overline{v}, \overline{w})$ are normalized by the channel half-width δ and the wall-friction velocity u_τ, which give the Reynolds number $Re_\tau = u_\tau \delta / \nu$ with the kinematic viscosity ν. Again, x, y and z denote the streamwise, the normal and the spanwise directions of the channel flow, respectively.

Each component of the GS velocities has the asymptotic form in the viscous sublayer ($y^+ = Re_\tau y < 5$) as follows:

$$\overline{u} = \langle \overline{u} \rangle + \overline{u}' = \langle \overline{u} \rangle + a_1(x,z,t)\, y + a_2(x,z,t)\, y^2 + \cdots, \tag{26}$$

$$\overline{v} = \overline{v}' = \qquad\qquad b_2(x,z,t)\, y^2 + \cdots, \tag{27}$$

$$\overline{w} = \overline{w}' = \qquad c_1(x,z,t)\, y + c_2(x,z,t)\, y^2 + \cdots, \tag{28}$$

where

$$\langle \overline{u} \rangle = Re_\tau \left(y - \frac{1}{2} y^2 + O(y^4) \right). \tag{29}$$

It is noted that the incompressibility condition requires the relation between a_1, b_2, and c_1

$$\frac{\partial a_1}{\partial x} + 2b_2 + \frac{\partial c_1}{\partial z} = 0. \tag{30}$$

From Eqs. (26), (27) and (28), the gradients of the GS velocities are

$$\frac{\partial \overline{u}}{\partial x} \sim \frac{\partial a_1}{\partial x} y\,, \quad \frac{\partial \overline{u}}{\partial y} \sim Re_\tau + a_1\,, \quad \frac{\partial \overline{u}}{\partial z} \sim \frac{\partial a_1}{\partial z} y\,,$$
$$\frac{\partial \overline{v}}{\partial x} \sim \frac{\partial b_2}{\partial x} y^2\,, \quad \frac{\partial \overline{v}}{\partial y} \sim 2b_2 y\,, \quad \frac{\partial \overline{v}}{\partial z} \sim \frac{\partial b_2}{\partial z} y^2, \tag{31}$$
$$\frac{\partial \overline{w}}{\partial x} \sim \frac{\partial c_1}{\partial x} y\,, \quad \frac{\partial \overline{w}}{\partial y} \sim c_1\,, \quad \frac{\partial \overline{w}}{\partial z} \sim \frac{\partial c_1}{\partial z} y\,,$$

where the $\sim$ means the leading-order-equality in a Taylor expansion with regard to $y \ll 1$. The following relations of the anisotropic filters width in channel flows are usually realized:

$$\overline{\Delta}_1 \approx \overline{\Delta}_3 \gg \overline{\Delta}_2\,, \qquad \widehat{\Delta}_1 \approx \widehat{\Delta}_3 \gg \widehat{\Delta}_2\,, \qquad \widehat{\overline{\Delta}}_1 \approx \widehat{\overline{\Delta}}_3 \gg \widehat{\overline{\Delta}}_2\,. \tag{32}$$

Let us evaluate the resolvable tensors L_{ij}, M_{ij}, $\mathcal{G}_{ij}$, and $\mathcal{H}_{ij}$. For the filtering in all directions (3-D filtering) , we assume the Gaussian or the top hat filter function.[11] Then a Taylor expansion of the fields $\overline{f}$ and $\overline{g}$ gives the following formulae

$$\widehat{\overline{f}} = \overline{f} + \frac{\widehat{\Delta}^2_{(a)}}{24} \frac{\partial^2 \overline{f}}{\partial x_{(a)} \partial x_{(a)}} + O(\widehat{\Delta}^4_{(a)})\,, \tag{33}$$

$$\widehat{\overline{fg}} - \widehat{\overline{f}}\,\widehat{\overline{g}} = \frac{\widehat{\Delta}^2_{(a)}}{12} \frac{\partial \overline{f}}{\partial x_{(a)}} \frac{\partial \overline{g}}{\partial x_{(a)}} + O(\widehat{\Delta}^2_a\, \widehat{\Delta}^2_b)\,, \tag{34}$$

$$\begin{aligned} O(\widehat{\Delta}^2_a\, \widehat{\Delta}^2_b) = {} & C_1\, \widehat{\Delta}^{\,2}_{(a)} \widehat{\Delta}^{\,2}_{(b)} \frac{\partial^2 \overline{f}}{\partial x^2_{(a)}} \frac{\partial^2 \overline{g}}{\partial x^2_{(b)}} + C_2\, \widehat{\Delta}^2_{(a)} \widehat{\Delta}^2_{(b)} \frac{\partial^2 \overline{f}}{\partial x_{(a)}\, \partial x_{(b)}} \frac{\partial^2 \overline{g}}{\partial x_{(a)}\, \partial x_{(b)}} \\ & + C_3\, \widehat{\Delta}^{\,2}_{(a)} \widehat{\Delta}^{\,2}_{(b)} \frac{\partial \overline{f}}{\partial x_{(a)}} \frac{\partial^3 \overline{g}}{\partial x_{(a)}\, \partial x^2_{(b)}} \\ & + C_4\, \widehat{\Delta}^{\,2}_{(a)} \widehat{\Delta}^{\,2}_{(b)} \frac{\partial^3 \overline{f}}{\partial x^2_{(a)} \partial x_{(b)}} \frac{\partial \overline{g}}{\partial x_{(b)}}\,, \end{aligned} \tag{35}$$

where C_1-C_4 are numerical constants. As mentioned in the next section, since the filtering and the derivatives are evaluated by the finite difference method with the fourth-order accuracy of the $\widehat{\Delta}$ or the mesh width in actual LES, the fourth-order terms derivable from the Taylor expansion are indistinguishable from the numerical truncation error. Hence, the important matter in Eq. (35) is not the numerical constants but the asymptotic behavior.

With the aid of Eqs. (14) and (33) - (35), we obtain

$$\mathcal{L}_{ij} \sim \left(\frac{\widehat{\Delta}^{\,2}_{(a)}}{12} \frac{\partial \overline{u}_i}{\partial x_{(a)}} \frac{\partial \overline{u}_j}{\partial x_{(a)}} \right)_\Sigma + O(\widehat{\Delta}^2_a\, \widehat{\Delta}^2_b)\,. \tag{36}$$

$$M_{ij} \sim 2\,\widehat{\Delta}^2\,|\overline{S}|\,\overline{S}_{ij} + O(\widehat{\Delta}^4), \tag{37}$$

$$\mathcal{G}_{ij} \sim \mathcal{H}_{ij} \sim -\left(\frac{\widehat{\Delta}_{(a)}^2}{12}\,\frac{\partial \overline{u}_i}{\partial x_{(a)}}\,\frac{\partial \overline{u}_j}{\partial x_{(a)}} \right)_{\Sigma} + O(\widehat{\Delta}_a^2\,\widehat{\Delta}_b^2). \tag{38}$$

Hence, Eqs. (36) and (38) give

$$\mathcal{L}_{ij} + \mathcal{G}_{ij} \sim \mathcal{L}_{ij} + \mathcal{H}_{ij} \sim O(\widehat{\Delta}_a^2\,\widehat{\Delta}_b^2). \tag{39}$$

From Eqs. (12), (13), (31), (32), and (36) - (39),

$$|\overline{S}| \sim Re_\tau + a_1, \tag{40}$$

$$\langle M_{ij}\,M_{ij}\rangle \sim 2\langle M_{12}^2\rangle \sim 2\,\widehat{\Delta}^4 Re_\tau^4, \tag{41}$$

$$\begin{aligned}
\langle\, \mathcal{L}_{ij} M_{ij}\,\rangle &\sim 2\,\langle\, \mathcal{L}_{12}\,M_{12}\,\rangle \\
&\sim -\frac{\widehat{\Delta}^2}{6}\left\langle \frac{\partial a_1}{\partial x}\,\frac{\partial b_2}{\partial x}\,\widehat{\Delta}_1^2 y^3 + 2a_1\,b_2\,\widehat{\Delta}_2^2 y + \frac{\partial a_1}{\partial z}\,\frac{\partial b_2}{\partial z}\widehat{\Delta}_3^2 y^3 \right\rangle Re_\tau^2, \\
&\sim -\frac{\widehat{\Delta}^2}{6}\left\langle \frac{\partial a_1}{\partial x}\,\frac{\partial b_2}{\partial x}\,\widehat{\Delta}_1^2 + \frac{\partial a_1}{\partial z}\,\frac{\partial b_2}{\partial z}\widehat{\Delta}_3^2 \right\rangle Re_\tau^2\, y^3,
\end{aligned} \tag{42}$$

$$\begin{aligned}
\langle (\mathcal{L}_{ij} + \mathcal{G}_{ij})\, M_{ij}\rangle &\sim C\,\widehat{\Delta}_a^2\,\widehat{\Delta}_b^2\,\widehat{\Delta}^2 Re_\tau^2\, y^3 \\
&\sim \left(C_5\widehat{\Delta}_1^4 + C_6\widehat{\Delta}_1^2\widehat{\Delta}_3^2 + C_7\widehat{\Delta}_3^4 \right) \widehat{\Delta}^2 Re_\tau^2\, y^3,
\end{aligned} \tag{43}$$

$$\begin{aligned}
\langle (\mathcal{L}_{ij} + \mathcal{H}_{ij})\, M_{ij}\rangle &\sim C'\widehat{\Delta}_a^2\,\widehat{\Delta}_b^2\,\widehat{\Delta}^2 Re_\tau^2\, y^3, \\
&\sim \left(C_8\widehat{\Delta}_1^4 + C_9\widehat{\Delta}_1^2\widehat{\Delta}_3^2 + C_{10}\widehat{\Delta}_3^4 \right) \widehat{\Delta}^2 Re_\tau^2\, y^3,
\end{aligned} \tag{44}$$

where C, C', and C_5 - C_{10} are numerical constants.

Now, we are ready to evaluate the model parameters from Eqs. (17), (19), (21), and (41) - (44) as follows:

$$C_{DSM} \sim \frac{1}{12}\left\langle \frac{\partial a_1}{\partial x}\,\frac{\partial b_2}{\partial x}\widehat{\Delta}_1^2 + \frac{\partial a_1}{\partial z}\,\frac{\partial b_2}{\partial z}\widehat{\Delta}_3^2 \right\rangle \frac{y^3}{\widehat{\Delta}^2 Re_\tau^2}, \tag{45}$$

$$C_{DCM} \sim \left(C_5\widehat{\Delta}_1^4 + C_6\widehat{\Delta}_1^2\widehat{\Delta}_3^2 + C_7\widehat{\Delta}_3^4 \right) \frac{y^3}{\widehat{\Delta}^2 Re_\tau^2}, \tag{46}$$

$$C_{DMM} \sim \left(C_8 \widehat{\Delta}_1^4 + C_9 \widehat{\Delta}_1^2 \widehat{\Delta}_3^2 + C_{10} \widehat{\Delta}_3^4 \right) \frac{y^3}{\widehat{\Delta}^2 Re_\tau^2}. \tag{47}$$

It is well known that the DSM is numerically stable with the positive C_{DSM}, which indicates the sign of the factor on the right-hand side of Eq. (45) as

$$\left\langle \frac{\partial a_1}{\partial x} \frac{\partial b_2}{\partial x} \widehat{\Delta}_1^2 + \frac{\partial a_1}{\partial z} \frac{\partial b_2}{\partial z} \widehat{\Delta}_3^2 \right\rangle < 0. \tag{48}$$

As it should be, C_{DSM} is asymptotic to y^3 in the vicinity of the wall. On the other hand, C_{DCM} with an isotropic filter shows negative value with the incorrect scaling of y [12], but Eq. (46) for an anisotropic filter shows the correct scaling of y^3 as mentioned in Ref. [13]. Eq. (46) is very similar to Eq. (47) , and both C_{DCM} and C_{DMM} have the same scaling of y^3. However, it is unknown without carrying out actual LES whether C_{DCM} and C_{DMM} near the wall are positive or not.

4. Numerical Evaluation by LES

Let us numerically check the above analytical results for a turbulent channel flow with $Re_\tau = 590$. For the DSM, the DCM, and the DMM we carry out LES with the grid-points $32 \times 64 \times 32$ and the computational domain $2\pi\delta \times 2\delta \times \pi\delta$ for numerical evaluation. The filtering and the derivatives are evaluated by the finite difference method with the fourth-order accuracy of the $\widehat{\Delta}$ or the mesh width. The time marching scheme is a third-order Adams-Bashforth method, and the coupling between the velocities and the pressure is calculated by the MAC scheme. The normalized time step is 1.0×10^{-5} and the statistics are obtained by averaging over 10 non-dimensional time units.

I also confirmed that LES for the DCM with an anisotropic filter can be carried out, although that with

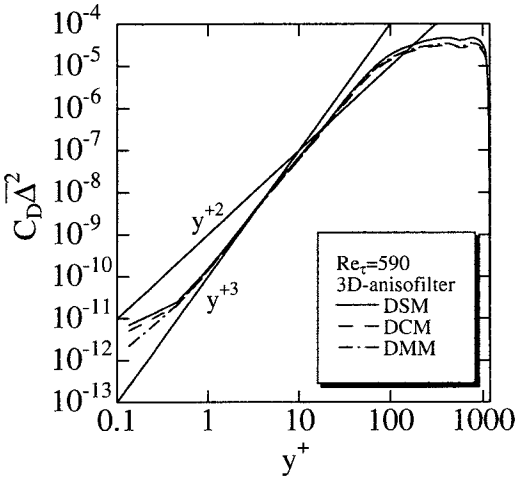

Fig.1 Asymptotic scalings of $C_D\overline{\Delta}^2$ for the DSM, the DCM, and the DMM near a wall.

an isotropic filter could not be carried out as mentioned before. Figure 1 shows the asymptotic behavior of $C_D\overline{\Delta}^2$ for the DSM, the DCM, and the DMM near the wall. The DCM with an anisotropic filter has the correct scaling of y^{+3}, although that with an isotropic filter has the scaling of y^{+}. The DCM with an anisotropic filter has the same scaling as the DSM and the DMM. All of these results agree with the analysis of the asymptotic behavior.

Figures 2, 3 and 4 how the profiles of the mean velocity, the shear stress, and the root mean square (rms) of the velocity fluctuations for the DSM, the DCM, and the DMM with the result of direct numerical simulation (DNS) [16], respectively. The profiles of the DCM and the DMM completely overlap each other, and the performance of both models are very similar. The mean velocity and the rms of the DSM are slightly overestimated in comparison with the others in Figs. 2 and 4. On the other hand,

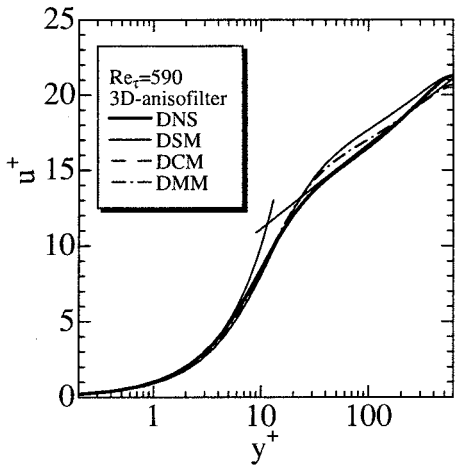

Fig.2 Mean velocity profiles for the DSM, the DCM, and the DMM.

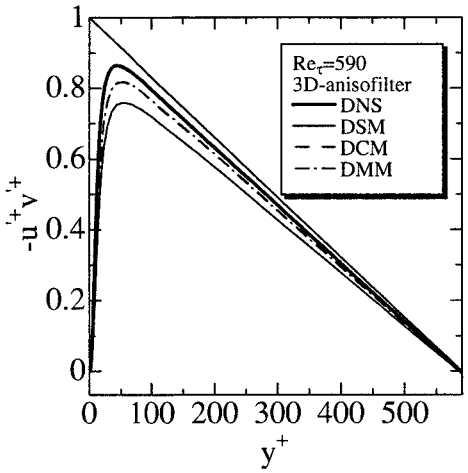

Fig.3 Profiles of the shear stress for the DSM, the DCM, and the DMM.

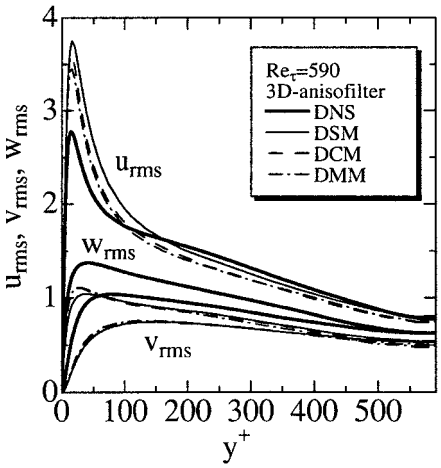

Fig.4 Profiles of the root mean square of the velocity fluctuations for the DSM, the DCM, and the DMM.

the shear stress of the DSM is underestimated in Fig. 3. This is why the DCM and the DMM indicate the higher performance than the DSM.

5. Conclusion

In the present paper, the near-wall scaling of the model coefficient for the DCM with an anisotropic filter has been revealed, then the performance of the DCM with an anisotropic filter, the DMM, and the DSM has been compared in actual LES. By improving the isotropic filter-width for the Clark term of the DCM into the anisotropic one, the DCM can be applied to turbulent channel flows. Then, the near-wall scaling of the model coefficient for the DCM is also corrected as y^3. The performance of the DCM is the almost same as that of the DMM.

Acknowledgments

The author would like to thank Prof. Y. Shimomura for his fruitful comments. This work is partially supported by the Keio Gijuku Academic Development Funds.

References

[1] R. S. Roggalo and P. Moin, "Numerical simulation of turbulent flows," Annu. Rev. Fluid Mech. **16**, 99 (1984) .

[2] M. Lesieur and O. Métais, "New trends in large-eddy simulations of turbulence," Annu. Rev. Fluid Mech. **28**, 45 (1996) .

[3] J. Smagorinsky, "General circulation experiments with the primitive equations. I. The basic

experiment,” Mon. Weather Rev. **91**, 99 (1963) .

[4] R. A. Clark, J. H. Ferziger, and W. C. Reynolds, “Evaluation of subgrid-scale models using an accurately simulated turbulent flow,” J. Fluid Mech. **91**, 1 (1979) .

[5] J. Bardina, J. H. Ferziger, and W. C. Reynolds, “Improved turbulence models based on LES of homogeneous incompressible turbulent flows,” Department of Mechanical Engineering, Report No. TF-19, Stanford (1984) .

[6] B. Vreman, B. Geurts, and H. Kuerten, “Large-eddy simulation of the temporal mixing layer using the clarkmodel,” Theoret. Comput. Fluid Dynamics **8**, 309 (1996) .

[7] B. Vreman, B. Geurts, and H. Kuerten, “Large-eddy simulation of the turbulent mixing layer,” J. Fluid Mech. **339**, 357 (1997) .

[8] M. Germano, U. Piomelli, P. Moin, and W. H. Cabot, “A dynamic subgrid-scale eddy viscosity model,” Phys. Fluids A **3**, 1760 (1991) .

[9] B. Vreman, B. Geurts, and H. Kuerten, “On the formulation of the dynamic mixed subgrid-scale model,” Phys. Fluids A **6**, 4057 (1994) .

[10] Y. Shimomura, “A family of dynamic subgrid-scale models consistent with asymptotic material frame indifference,” J. Phys. Soc. Jpn. **68**, 2483 (1999) .

[11] H. Kobayashi and Y. Shimomura, “The performance of dynamic subgrid-scale models in the large eddy simulation of rotating homogeneous turbulence,” Phys. Fluids **13**, 2350 (2001) .

[12] H. Kobayashi and Y. Shimomura, “Inapplicability of the dynamic Clark model to the large eddy simulation of incompressible turbulent channel flows,” Phys. Fluids **15**, L29 (2003) .

[13] A. W. Vreman, “Comment on “Inapplicability of the dynamic Clark model to the large eddy simulation of incompressible turbulent channel flows”,” Phys. Fluids **16**, 490 (2004) .

[14] H. Kobayashi and Y. Shimomura, “Response to “Comment on ‘Inapplicability of the dynamic Clark model to the large eddy simulation of incompressible turbulent channel flows’ ”,” Phys. Fluids **16**, 492 (2004) .

[15] D. K. Lilly, “A proposed modification of the germano subgrid-scale closure method,” Phys. Fluids A **4**, 633 (1992) .

[16] R. D. Moser, J. Kim, and N. N. Mansour, “Direct numerical simulation of turbulent channel flow up to $Re_\tau = 590$,” Phys. Fluids **11**, 943 (1999) .